REPORT DOCUMENTATION PAGE

1. REPORT DATE (DD-MM-YYYY)	2. REPORT TYPE	3. DATES COVERED (From - To)
25-06-2003	Technical Paper	

4. TITLE AND SUBTITLE

Investigation of Operation and Characteristics of Small SPT with Discharge Chamber Walls Made of Different Ceramics

5a. CONTRACT NUMBER

5b. GRANT NUMBER

5c. PROGRAM ELEMENT NUMBER

6. AUTHOR(S)

V. Kim, A. Skrylnikov, A. Veselovzorov (Russian Scientific Center Kurchatov Institute); J. Michael Fife (AFRL/PRSS); Summer C. Locke (Univ. of Washington)

5d. PROJECT NUMBER
2308

5e. TASK NUMBER
M4S7

5f. WORK UNIT NUMBER

7. PERFORMING ORGANIZATION NAME(S) AND ADDRESS(ES)

Air Force Research Laboratory (AFMC)
AFRL/PRSS
1 Ara Drive
Edwards AFB CA 93524-7013

8. PERFORMING ORGANIZATION REPORT NUMBER

AFRL-PR-ED-TP-2003-174

9. SPONSORING / MONITORING AGENCY NAME(S) AND ADDRESS(ES)

Air Force Research Laboratory (AFMC)
AFRL/PRS
5 Pollux Drive
Edwards AFB CA 93524-7048

10. SPONSOR/MONITOR'S ACRONYM(S)

11. SPONSOR/MONITOR'S NUMBER(S)

AFRL-PR-ED-TP-2003-174

12. DISTRIBUTION / AVAILABILITY STATEMENT

Approved for public release; distribution unlimited.

13. SUPPLEMENTARY NOTES

For presentation at the AIAA Joint Propulsion Conference in Huntsville, AL, 20-23 July 2003.

14. ABSTRACT

20030812 158

15. SUBJECT TERMS

16. SECURITY CLASSIFICATION OF:			17. LIMITATION OF ABSTRACT	18. NUMBER OF PAGES	19a. NAME OF RESPONSIBLE PERSON Leilani Richardson
a. REPORT	b. ABSTRACT	c. THIS PAGE	A	11	19b. TELEPHONE NUMBER (include area code)
Unclassified	Unclassified	Unclassified			(661) 275-5015

INVESTIGATION OF OPERATION AND CHARACTERISTICS OF SMALL SPT WITH DISCHARGE CHAMBER WALLS MADE OF DIFFERENT CERAMICS

Vladimir Kim, Vyacheslav Kozlov, Alexander Skrylnikov, Alexander Veselovzorov
Russian Scientific Center "Kurchatov Institute", Moscow, Russia
John M. Fife
United States Air Force AFRL/PRSS, Edwards AFB, CA, USA
Summer C. Locke
University of Washington, Seattle, WA, USA

Abstract

There was made characterization of the SPT-25 model with discharge chamber walls made of different materials such as the Russian BN-SiO$_2$ (BGP) type ceramics, AlN-BN and BN types ceramics produced in France and in USA, respectively. The 1st one is used in a modern SPT-70 and SPT-100 flight designs and two other ones are the prospective materials for SPT discharge chamber manufacturing. These materials have good enough properties under increased temperatures. It is interesting also that according to published data they have different secondary electron emission. So, characterization of thruster with the discharge chamber wall made of the mentioned materials could give some indications of the secondary electron emission influence on thruster operation and performance.

The SPT-25 model has external accelerating channel diameter 25mm and acceptable performance level under discharge powers (100-200)W. To characterize its operation with discharge chamber walls made of different ceramics there were determined the voltage-current characteristics of the mentioned model under different magnetic fields inside the accelerating channel and different mass flow rates through the accelerating channel. There were determined also the thrust values and other output parameters such as the thrust efficiency and specific impulse, the accelerated ion flow divergence by measurement of the accelerated ion current distributions in off-axis angle by RPA probe, some plume plasma parameters measured by cylindrical electrostatic probe and discharge voltage and current oscillation characteristics.

Obtained results confirm high enough performance level of the SPT-25 model with BGP ceramics. It has demonstrated the total thrust efficiency (calculated accounting for the cathode mass flow rate and power losses for magnetization) ~0,25 and specific impulse ~885s under power ~100W, the total thrust efficiency ~0,32 and specific impulse ~1300s under power ~200W. There was obtained also complex of thruster integral characteristics allowing comparison of these characteristics for different discharge chamber materials. In particular there was found notable difference of voltage-current characteristics and thrust values for different ceramics under low mass flow rates and magnetic fields. Moreover thrust and thrust efficiency are different with different materials even under very close discharge voltages and currents obtained under comparable conditions and great enough magnetic fields. Thus, there was obtained more or less complex information allowing comparison of thruster characteristics with discharge chamber walls made of different materials.

Introduction.

It was known already many years, at least in Russia, that the discharge chamber material has great impact on the SPT operation, characteristics and performance level[1-4] and there was found that such ceramics as AlN-BN, BN and BN-SiO$_2$ having good enough general properties (high enough mechanical strength, low electric conductivity under increased temperatures and low sputtering yield under ceramics bombardment by ions, high breakdown electric field intensity, heat resistance and resistance to the mechanical and thermal shocks etc.) are acceptable for the discharge chamber manufacturing. It was clear also that significant role has to play the ceramics secondary electron emission[2,3] due to its possible impact at least on the near wall Debay sheath thickness and potential drop, electron energy balance and so-called near wall conductivity. But there was not made systematic study of this specific ceramics property influence on thruster operation and characteristics. Therefore some studies in this direction fulfilled last years[5-11] are reasonable and to be continued because even by now there is no experimental data clearly and quantitatively showing role of the secondary electron emission in the SPT discharge. The main reasons of such situation are the complexity of processes in SPT, difficulty of the near wall processes experimental study due to small sizes of the Debay sheath and lack of information on physical conditions at dielectric wall surfaces contacting with plasma and some ceramics properties such as the secondary electron emission yield (SEEY). Therefore it is reasonable to continue

experimental study of operation peculiarities and characteristics of SPTs with discharge chamber walls made of different materials as well as to realize studies of the ceramics properties influence on processes in SPT with usage of some SPT discharge theoretical models taking into account the plasma-wall interaction. Surely it is difficult to develop the adequate discharge model, if there are some unsolved questions on the plasma-wall interaction. Nevertheless this is one of the possible ways to get the final success and determination of maximum information on thruster characteristics with different discharge chamber wall materials could extend the data base for verification of different discharge models. Taking all the mentioned into account there was made characterization of the SPT-25 model with discharge chamber walls made of AlN-BN produced by MCSE in France, of the BN ceramics produced in USA and of the BN-SiO$_2$ (or BGP) ceramics produced in Russia and used in the modern SPT-70 and SPT-100 designs. The last material was used as the basic one for the comparative characteristics study. In parallel there is going work at CERN on determination of SEEY for the same materials which is not finished. But according to published data[10] the SEEY levels are different for the mentioned ceramics. So, obtained characteristics could be used for analysis of the SEEY influence on thruster operation and performance.

It is necessary to add that the detailed SPT-25 model characterization is interesting itself because this model has acceptable performance level under operation at powers ~100W[12]. Results of the mentioned characterization are represented in the paper.

1. Methodology of the SPT-25 characterization.

As it was mentioned above for this study there was used the SPT-25 type thruster model[12] (Fig.1) having an external accelerating channel diameter 25 mm and magnetic system with one magnetization coil. Advantage of such model is mainly radial direction of magnetic field lines (Fig.2) and small variation of the magnetic field topology under variation of magnetic field to optimize the operation mode. Direct measurements of the magnetic field intensity along the accelerating channel mid surface show that the SPT-25 magnetic system was able to create great enough magnetic field and there was some indications of the magnetics saturation under magnetization currents over 3A (Fig.3). Discharge chamber wall exit parts (see Fig.1) were made as replacable circular rings. So, it was possible to manufacture these rings of different materials and to replace them. As it was mentioned above as the basic option there was used the BGP type ceramics. Therefore for this material there was made full enough characterization. Other options of the discharge chamber walls were manufactured of the AlN-BN and BN samples produced in USA. Thruster geometry and sizes of parts were identical for all materials within the manufacturing accuracy.

SPT-25 model was tested inside the vacuum chamber of 2m in diameter and 6m in length. This chamber was equipped by thrustmeter having accuracy of measurements ±3 percents within the range of the thrust values 5-10 mN. Test facility has also system supplying gas (Xe) into the accelerating channel through anode and into cathode as well as power supply sources for all thruster circuits and electric parameters measuring system. The mass flow rate through anode was controlled and measured with accuracy ± 3 percents within the range of (0,5-1)mg/s and cathode mass flow rate-with accuracy of ± 5 percents under its value ~0,1mg/s. The dynamic pressure during the SPT-25 tests with mass flow rates through thruster ~1 mg/s and less did not exceed $1.5 \cdot 10^{-5}$ Torr by Xe.

Test facility was equipped also by the system of the accelerated ion flow parameters measurement allowing determination of the accelerated ion current distribution along the semicircle with the center positioned at the thruster exit and with circle plane consisting of the thruster axis. To realize these measurements there was used the RPA probe mounted on the boom rotating along the mentioned semicircle within ± 90 degrees relative to the thruster axis. This system allows determination of the accelerated ion current distribution in off-axis direction, angular distribution of accelerated ions energy and estimation of thruster plume divergence.

To characterize the thruster model there were measured discharge current and thrust under different currents in magnetization coil for several fixed mass flow rates through anode and several fixed discharge voltage values. The range of mass flow rates through anode was (0,5-1,0) mg/s. The discharge voltage was varied within (125-250)V. Thus, it was possible to determine the possible discharge chamber material impact on the voltage-current characteristics, dependence of discharge current on magnetic field intensity as well as to determine thrust and thrust efficiency under different discharge conditions. There was also made the discharge voltage and current oscillations preliminary characterization, namely: to estimate the discharge voltage and current oscillations intensity there were registered their (5-10) occasional traces by digital oscilloscope. Then there were realized their Fourier-analysis within the range of frequencies 0-250 kHz and calculation of the mean RMS amplitudes of the discharge voltage and current oscillations for 50 harmonics as well as determination of the dominating oscillation frequency.

It is necessary to note that for the 1st series of tests on the SPT-25 characterization with BGP ceramics and with AlN-BN ceramics there was used heaterless cathode specially designed for small SPT's at Kharkov Aviation Institute. But this cathode (cathode #1) was broken after these tests. Therefore the second series of tests was made with usage of another cathode (cathode #2) designed for the SPT-100 which was oversized for the SPT-25 model. Particularly it was

difficult to operate it under discharge currents lower than 1A. Taking this into account there was used its additional heating by power ~25 W, but even in this case the SPT-25 thrust and thrust efficiency (calculated not accounting for cathode losses) were lower than in the 1st series. Nevertheless all characteristics were repeatable. Therefore there was made comparative study of the SPT-25 characteristics with BGP and BN type ceramics with the second cathode (cathode #2) but theses data are to be considered as the preliminary ones. To distinguish all the tested cases below there will be used the following notations for the tested options:

option number	ceramics	cathode
#1	BGP	#1
#2	BGP	#2
#3	AlN-BN	#1
#4	BN	#2

The angular accelerated ion current distributions were determined under retarding potential Ur=+50V relative to cathode potential. Because plasma potential in a plume was ~ 20V under such retarding potential the RPA collector current is created by ions with energies higher than ~30eV. Thus, usage of the mentioned retarding potential value allows characterization only ions in a plume able to have notable mechanical, thermal and erosion impacts on surfaces crossed by plume.

For the basic option there were determined the plasma parameter distributions in a small SPT plume under its operation with discharge power ~100W and ~200W. To measure these parameters in addition to RPA there was used cylindrical Langmuir probe with axis oriented to thruster exit and mounted on the mentioned rotating boom. Due to existence of the accelerated ions in a plasma it is difficult to have satisfactory interpretation of probe characteristics. Experience coupled by authors of this paper shows that probe characteristics close to classical one could be obtained with cylindrical probe oriented as it was mentioned above. To verify this conclusion there were made special measurements with usage of cylindrical probe and emissive probe. These measurements gave satisfactory agreement of the plasma potential values measured by emissive probe and derived from probe characteristics obtained by cylindrical probe. Plasma parameters in a SPT-25 plume were determined at three distances of probes from the thruster exit, namely: along the semicircles with radiuses R=0,3m, R=0,4m and R=0,5m. Sensitivity of measuring system did not allow obtaining of reliable data at larger distances.

2. Results of the SPT-25 characterization with discharge chamber walls made of BGP(option #1)

Results of the SPT-25 option #1performance characterization (Fig.4-9) show that:

1. Model has typical for SPT characteristics under great enough magnetic induction and there is saturation of thruster performance under high enough magnetization currents (see Fig.6 and Fig.9). It is possible to conclude also that under magnetization currents Im $\geq$ (2,5-3)A there is no further increase of the thrust efficiency with increase of the magnetization current. So, the mentioned values could be considered as optimal ones. It is necessary to add that the mentioned characteristics were determined while magnetization current was reduced from high values till low ones to reduce impact of the thruster model overheating taking place under low magnetization currents while discharge current is great.

2. There is confirmed the possibility to obtain acceptable total thrust efficiency of the SPT-25 model with discharge chamber walls made of BGP under its operation with discharge power Nd~100W and good enough performance level under discharge power Nd~200W (Table 1).

Table 1. Operation mode parameters and performance data

	Mode 1	Mode 2
anode mass flow rate, mg/s	0.6	0.7
cathode mass flow rate, mg/s	0.1	0.1
discharge voltage, V	151	224
discharge current, A	0.64	0.86
discharge power, W	96.7	192.6
thrust, mN	6.0	10.2
total power consumption, W	103.7	200.7
total specific impulse, s	885	1299
total thrust efficiency, %	0.253	0.324
plume half angle for 95% of accelerated ions, degrees	79	66

3. Data obtained by RPA and cylindrical probe allow the following conclusions:

- the plume half angle values for the 95% of measured current were within the range of 65-80 degrees and this angle is reduced with increase of discharge voltage and magnetization current;

- mean energy of ions is reduced significantly only under off-axis angles higher than 45-50 degrees and the difference between discharge voltage and mean ion energy maximum is almost the same under Ud=150V and Ud=225V ;

- plasma potential distributions has maximum in vicinity of thruster axis and level of potential is (20-22)V ;

- electron temperature is at level of ~1eV and also slightly increased in direction to the thruster axis ;

- plasma potential and electron temperature are not changed significantly with increase of distance from the thruster exit.

The oscillation characteristics will be discussed below.

3. Comparative study of the SPT-25 characteristics with different cathodes and discharge chamber wall materials

Characteristics of the SPT-25 options #1 and #2.

As it was mentioned above the characteristics of the SPT-25 options #1 and #2 are significantly different. In particular the discharge current and thrust are typically lower with cathode #2 (Fig.10-18). Finally the thrust efficiency (calculated not accounting for cathode mass flow rate and additional heating power with cathode #2) is significantly lower than with cathode #1. This is an indication of fact that SPT-25 is very sensitive to the cathode operation. Probably, the mentioned characteristics behavior is caused by difference of the electron temperatures at the exit of different cathodes and different probability of the gas flow ionization causing difference of the ion and discharge currents, but this point is to be studied additionally.

Difference in thruster operation is confirmed also by difference of the oscillation characteristics (Fig. 19-21).

Characteristics of the SPT-25 options #1 and #3

The SPT-25 model option #3 (with discharge chamber walls made of AlN-BN and cathode #1) characteristics are qualitatively similar to that ones obtained for the option #1(Fig.22-33) but under low mass flow rate and magnetization currents the discharge current is typically higher (see Fig. 22) and thrust is typically lower (see Fig.23). More over even under close discharge currents realized under high enough magnetization currents thrust in this case is also lower (see Fig. 24-26). That is why the thrust efficiency in the case of AlN-BN ceramics is lower (see Fig. 27). It is necessary to add that the range of the stable operation modes for AlN-BN case is more narrow, probably, due to reduction of the thrust efficiency.

So, there was found the definite difference of integral characteristics for the AlN-BN case in comparison with basic case. It is necessary to add that in this case under discharge voltages Ud~200V or higher there were appeared the breakdowns between anode and internal magnetic pole of the magnetic system creating hole (channel) with almost circular cross-section in internal discharge chamber exit ring body and having mainly axial direction of the hole axis.

Characteristics of the SPT-25 option #3 and option #4

Comparison of these options characteristics shows that:
- as in the case of AlN-BN/BGP pair there are some differences in voltage-current characteristics under low magnetic fields in the case of BGP/BN pair

and with increase of magnetic field these differences become negligible;
- in the case of BN the discharge current under low magnetic fields is typically a little bit higher and thrust is a little bit lower than in BGP case, therefore the thrust efficiency under low magnetic fields is lower in the BN case, but under high enough magnetic fields the thrust and thrust efficiency are practically the same;
- the plume divergence behavior is similar in both cases;
- the oscillation characteristics are significantly different for significant part of the operation modes and have no direct link with the discharge current behavior;
- dependencies of integral parameters on magnetization current for the BN case are qualitatively the same as for the AlN-BN and BGP.

4. Preliminary discussion of the obtained results

As a whole obtained results confirm that SPT-25 model has acceptable performance level under low powers and that SPT characteristics depend on the discharge chamber material as well as on the specific thruster and cathode designs and their operation modes. They confirm also once more the complexity of processes in SPT.

Concerning the secondary electron emission influence on thruster operation and performance one can conclude that there is no simple or clear correlation between the level of the SEEY and thruster operation and performance. Indeed, according to published data the BGP SEEY level is intermediate between SEEY of the AlN-BN and BN. The relationship of the discharge current, thrust and thrust efficiencies under low magnetic fields for the tested three materials are not in correspondence with the mentioned trend. So, as at the beginning of paper one can conclude that studies in the considered direction are to be continued including the SEEY determination which is, probably, to be done for the samples manufactured from the same piece of material which was used for the concrete discharge chamber manufacturing. The last conclusion follows from preliminary results obtained at CERN for the considered materials which are significantly different from published ones.

Conclusion

As a result of the represented work there were obtained new data on the discharge chamber material influence on the SPT operation and characteristics showing the necessity of further studies to get clear understanding of some specific ceramics properties influence on the mentioned characteristics including influence of the secondary electron emission yield.

Acknowledgements

References

1. A. I. Morozov, in: Plazmennye Uskoriteli (in Russian, edited by L.A. Artsimovich), Mashinostroenie, Moscow, 1973, p.p. 85-92.

2. A.I. Morozov. Physical bases of the Electric Propulsion. V.1. Elements of flow dynamics in Electric Propulsion (in Russian), Atomizdat, Moscow, 1978, p.p. 213-220.

3. V.A. Smirnov. Electron energy balance in accelerators with closed drift of electrons and extended acceleration zone (ACDE) (in Russian) - Physika Plazmy, v.5, #2, 1979, p.p. 361-367.

4. V.V. Egorov, V.Kim, A.A. Semenov, I.I. Shkarban, in: Ionnye Inzhectory i Plasmennye Uskoriteli(in Russian, edited by A.I. Morozov and N.N. Semashko), Energoatomizdat, Moscow, 1990, p.p. 56-68.

5. K.N.Kozubskii, V.M. Murashko, Yu.P. Rylov et. al. Stationary Plasma Thrusters operate in Space-Plasma Physics Reports, v.29, #3, 2003, p.p. 251-266.

6. L. Jolivet, J.-F. Roussel. Effects of the secondary electron emission on the sheath phenomenon in a Hall Thruster-Proceedings of 3rd International Spacecraft Propulsion, 10-13 October 2000, Cannes, France, p.p. 367-384.

7. S. Locke, U. Shumlak, J.M. Fife. Numerical study of the Effect of channel insulator discontinuity on Hall thruster discharge-paper IEPC-01-23, 27th IEPC, October 15-19, 2001, Pasadena, CA, USA.

8. S. Barral, K. Makovski, Z. Peradzinski, N. Gascon, M.Dudeck-paper AIAA 2002-4245, 38th JPC, 7-10 July 2002, Indianapolis, IN, USA.

9. E. Ahedo, F.I. Parra. Model of radial plasma-wall interactions in a Hall thruster discharge-paper AIAA 2002-4106, 38th JPC, Indianapolis, IN, USA.

10. V.Viel-Inguimbert. Secondary electron emission of ceramics used in the channel of SPT-paper IEPC–03-258, 28th EPC, 17-21 March 2003, Toulouse, France.

11. E. Raitses, A. Dunaevsky, N. Fish. Yield of the secondary electron emission from ceramics materials of Hall thrusters with segmentd electrodes-paper IEPC-03-164, 28th IEPC, 17-21 March 2003, Toulouse, France.

12.B. Arkhipov, V. Kim, V.I. Kozlov et al. , in: Proceedings of 3rd International Spacecraft Propulsion, 10-13 October, 2000, Cannes, France, p.p. 399-401.
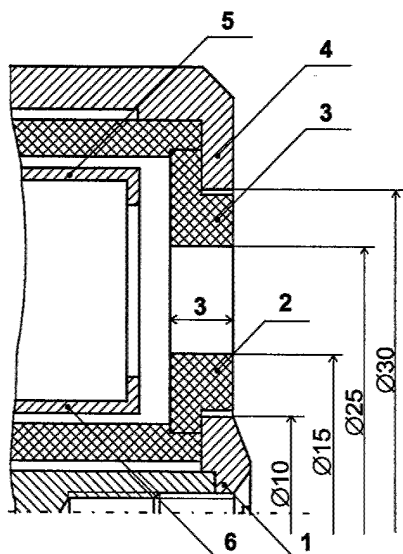
Fig. 1. SPT-25 exit part diagram.
1 – internal magnetic pole;
2 – internal ceramic ring;
3 – external ceramic ring;
4 - external magnetic pole;
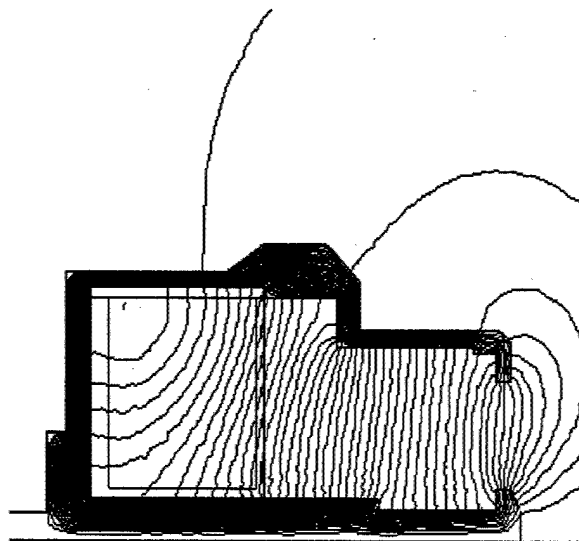5 – external anode ring;
6 - internal anode ring.
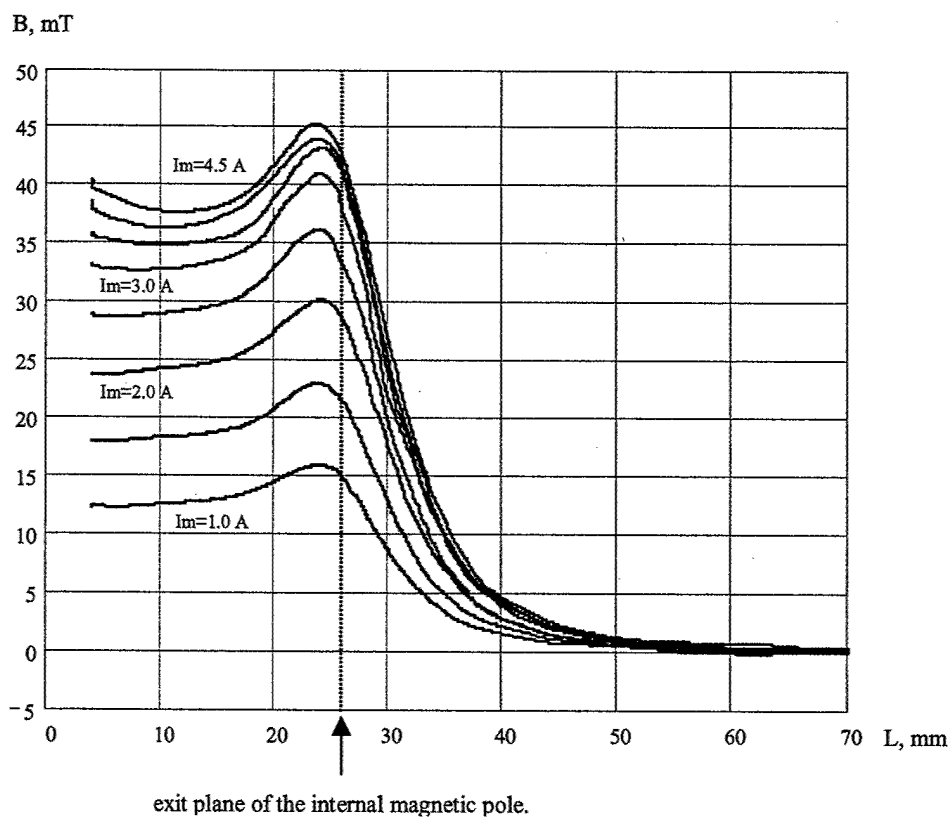

Fig. 2. The SPT-25 magnetic field topology
(Im=2.5 A).

B, mT

exit plane of the internal magnetic pole.

Fig. 3. The radial magnetic field distribution along the accelerating channel mid surface.

SPT-25 #1, m$_a$=0.6 mg/s

Id, A
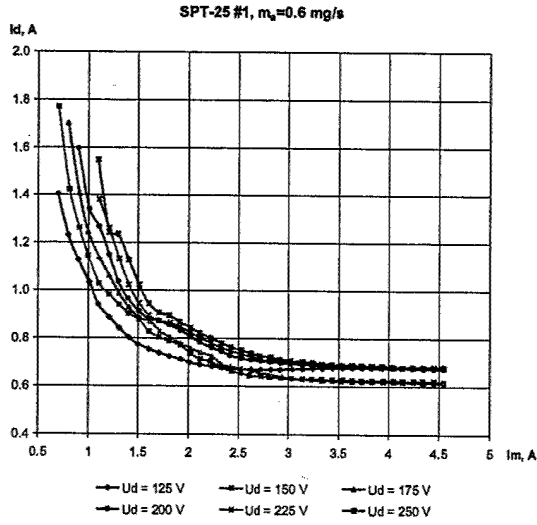
Fig. 4. Discharge current versus the magnetization current.

SPT-25 #1, m$_a$=0.8 mg/s

Id, A
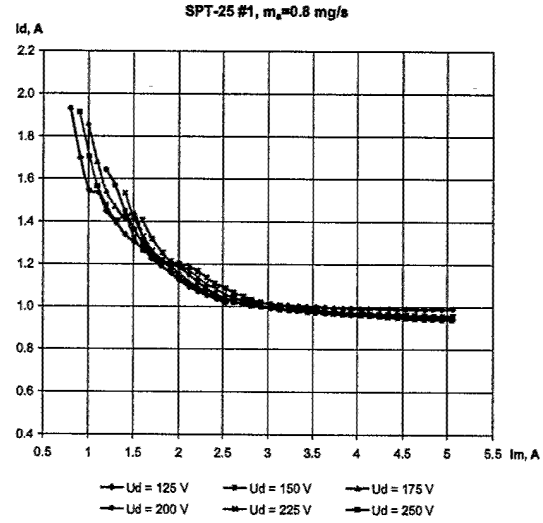
Fig. 7. Discharge current versus the magnetization current.

SPT-25 #1, m$_a$=0.6 mg/s

T, mN
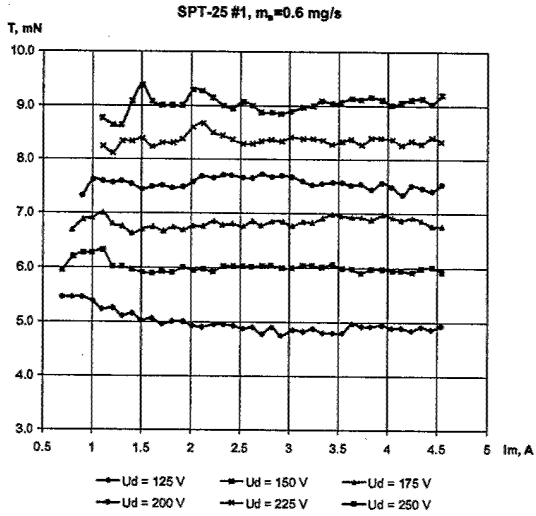
Fig. 5. Thrust versus the magnetization current.

SPT-25 #1, m$_a$=0.8 mg/s

T, mN
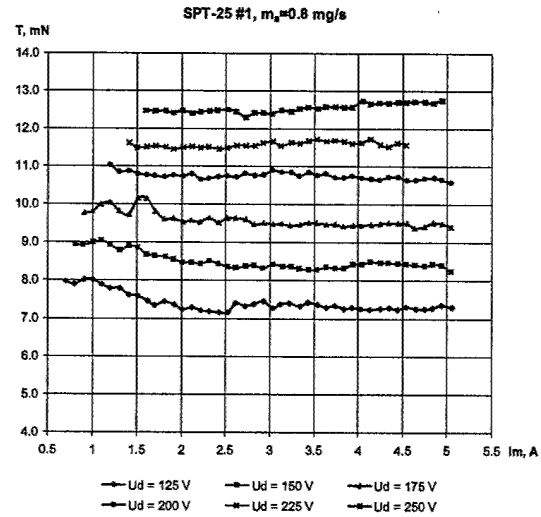
Fig. 8. Thrust versus the magnetization current.

SPT-25 #1, m$_a$=0.6 mg/s

η_{ta}
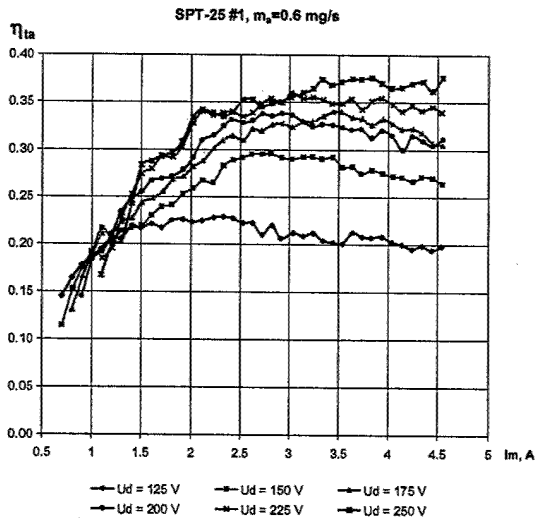
Fig. 6. Thrust efficiency versus the magnetization current.

SPT-25 #1, m$_a$=0.8 mg/s

η_{ta}

Fig. 9. Thrust efficiency versus the magnetization current.

7

American institute of Aeronautics and Astronautics

SPT-25, Im=1.5 A
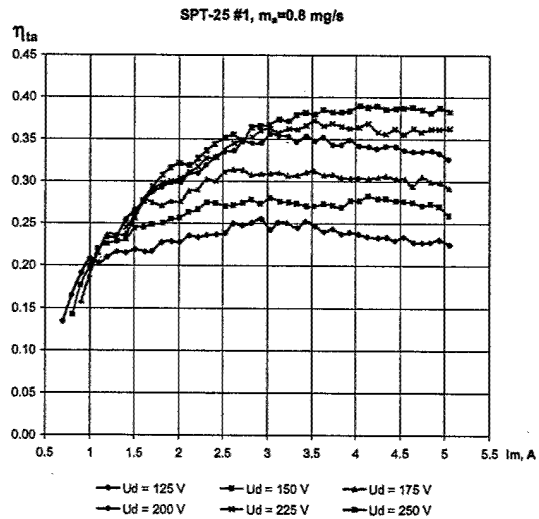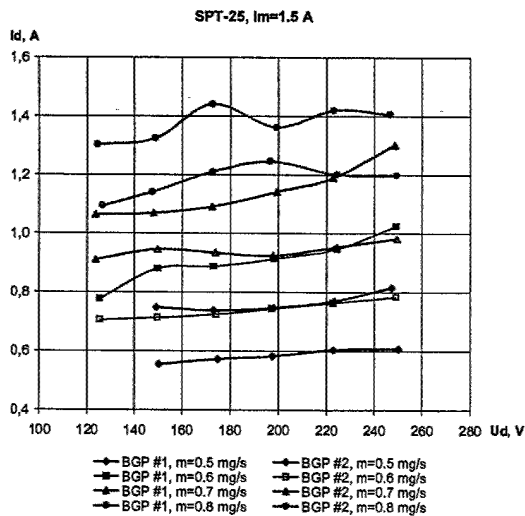
Fig. 10. Voltage-current characteristics with cathode #1 and cathode #2.

SPT-25, Im=1.5 A
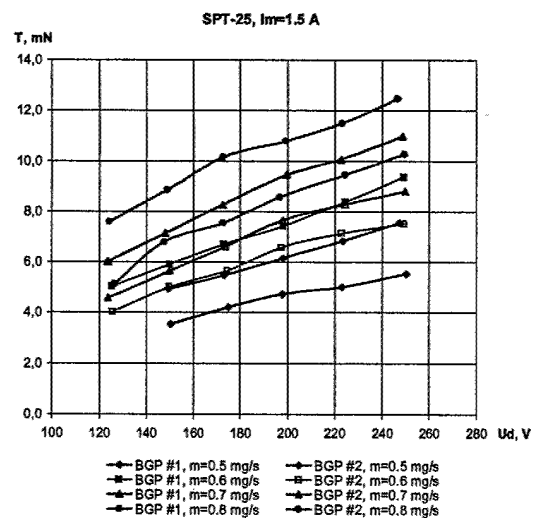
Fig. 13. Thrust versus the discharge voltage with cathode #1 and cathode #2.

SPT-25, Im=2.5 A
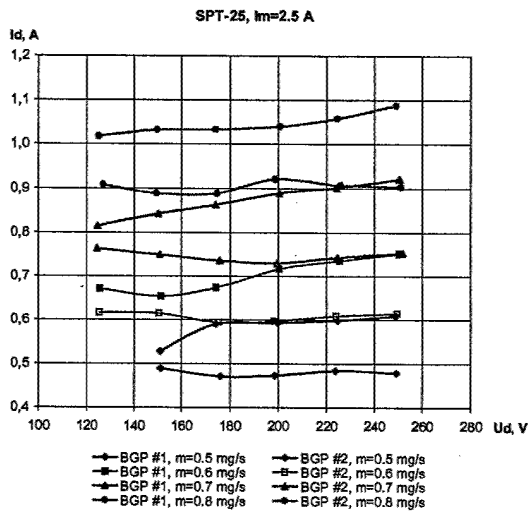
Fig. 11. Voltage-current characteristics with cathode #1 and cathode #2.

SPT-25, Im=2.5 A
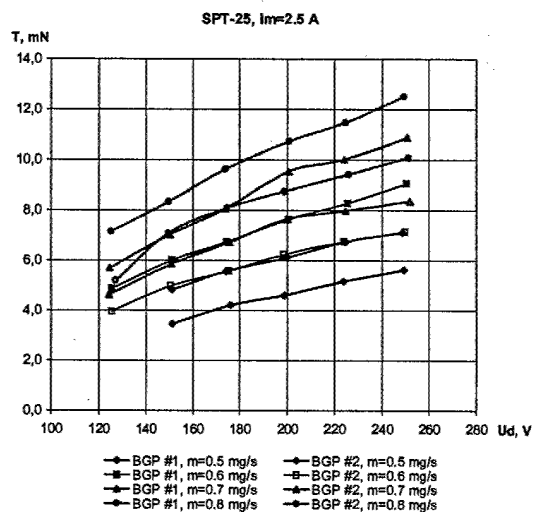
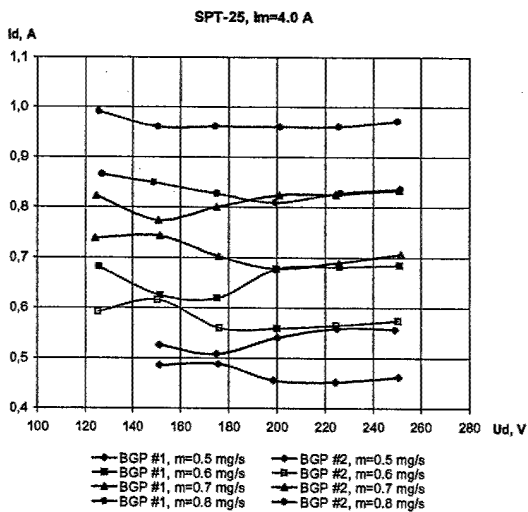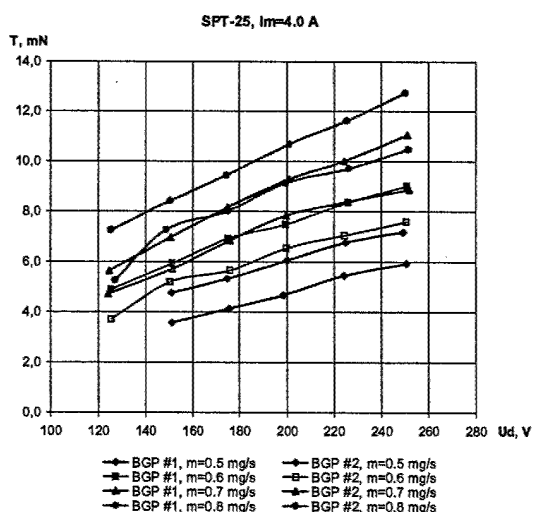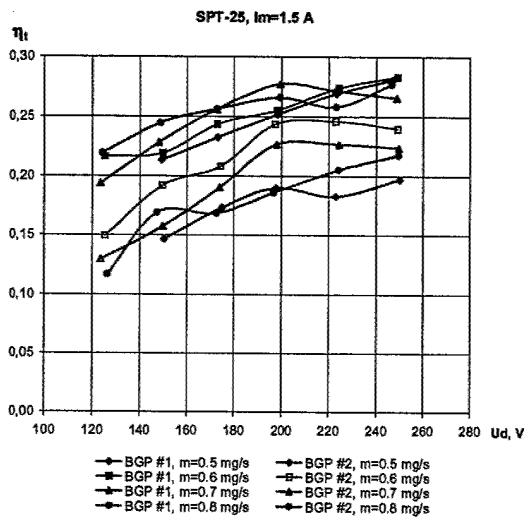Fig. 14. Thrust versus the discharge voltage with cathode #1 and cathode #2.

SPT-25, Im=4.0 A

Fig. 12. Voltage-current characteristics with cathode #1 and cathode #2.

SPT-25, Im=4.0 A

Fig. 15. Thrust versus the discharge voltage with cathode #1 and cathode #2.

8

SPT-25, Im=1.5 A

Fig. 16. Thrust efficiency versus the discharge voltage with cathode #1 and cathode #2.

SPT-25, m=0.6 mg/s, Im=1.5 A.

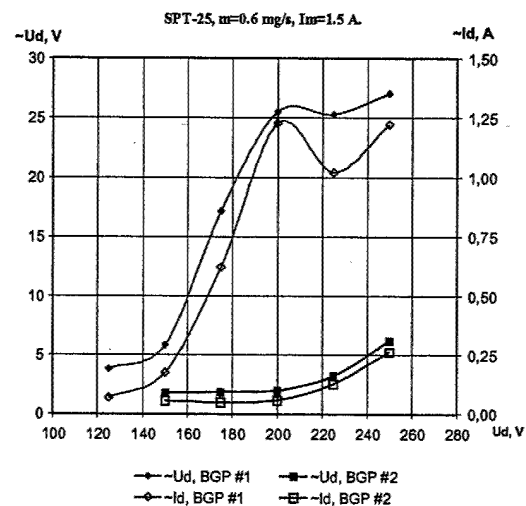Fig. 19. The discharge voltage and current RMS amplitude versus the discharge voltage with cathode #1 and cathode #2.
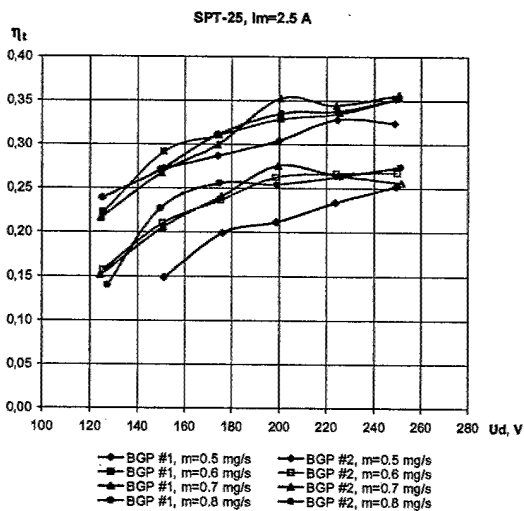
SPT-25, Im=2.5 A

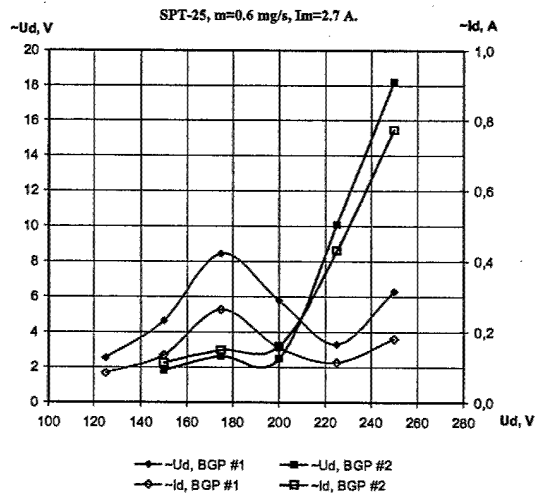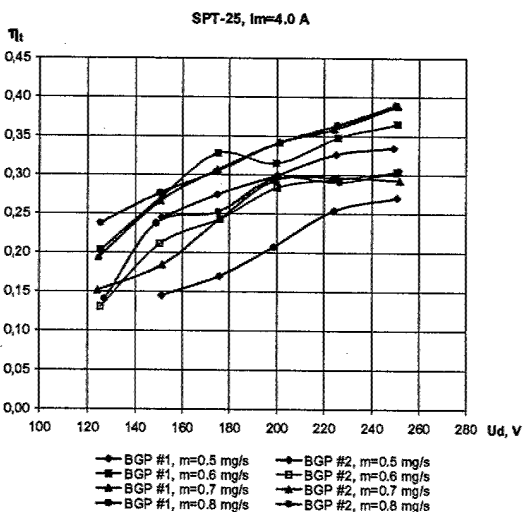Fig. 17. Thrust efficiency versus the discharge voltage with cathode #1 and cathode #2.

SPT-25, m=0.6 mg/s, Im=2.7 A.

Fig. 20. The discharge voltage and current RMS amplitude versus the discharge voltage with cathode #1 and cathode #2.

SPT-25, Im=4.0 A

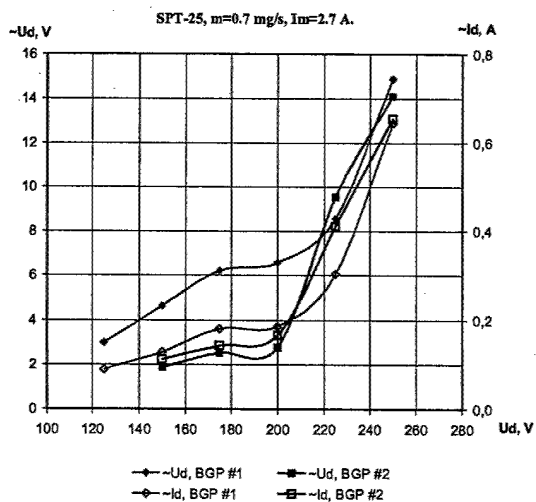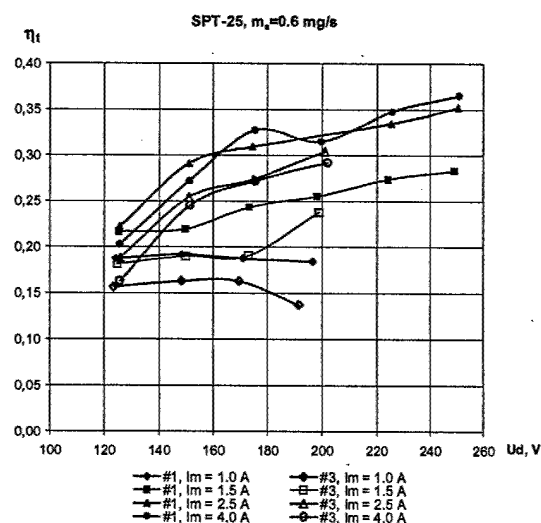Fig. 18. Thrust efficiency versus the discharge voltage with cathode #1 and cathode #2.

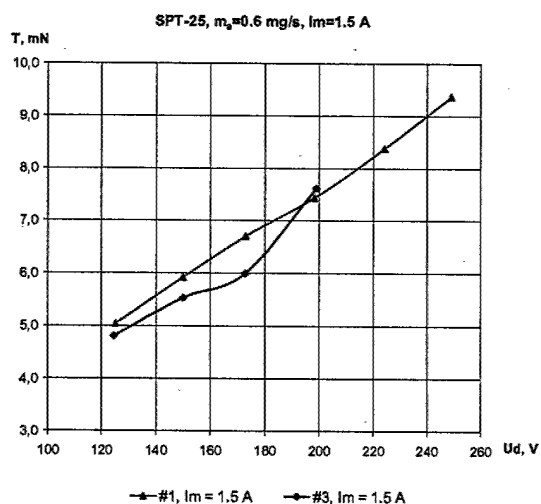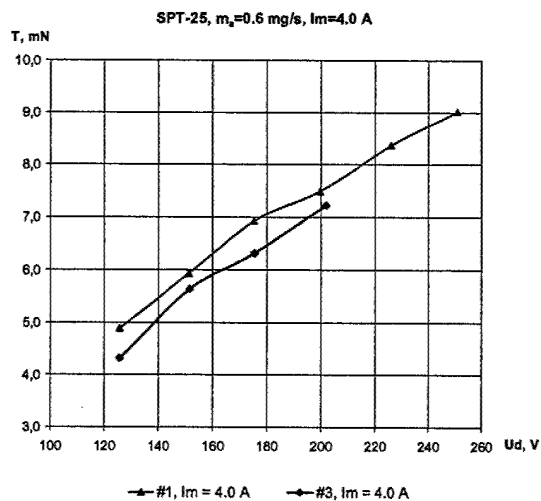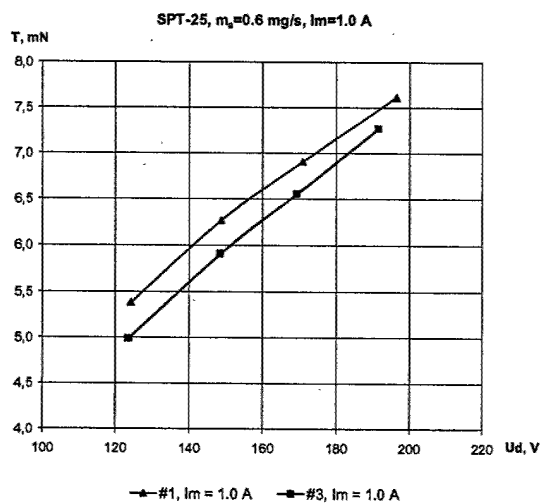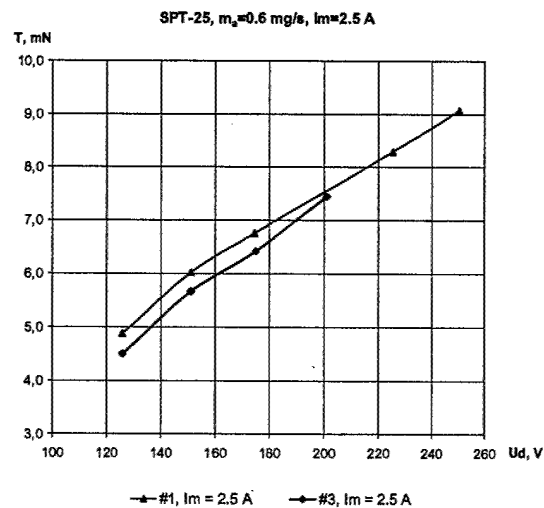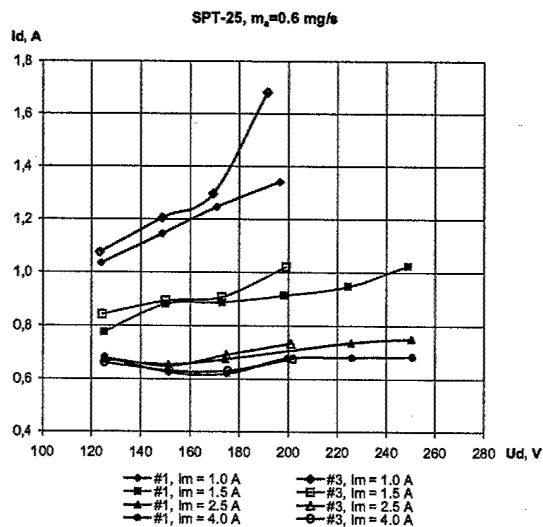**SPT-25, m=0.7 mg/s, Im=2.7 A.**

Fig. 21. The discharge voltage and current RMS amplitude versus the discharge voltage with cathode #1 and cathode #2.

9

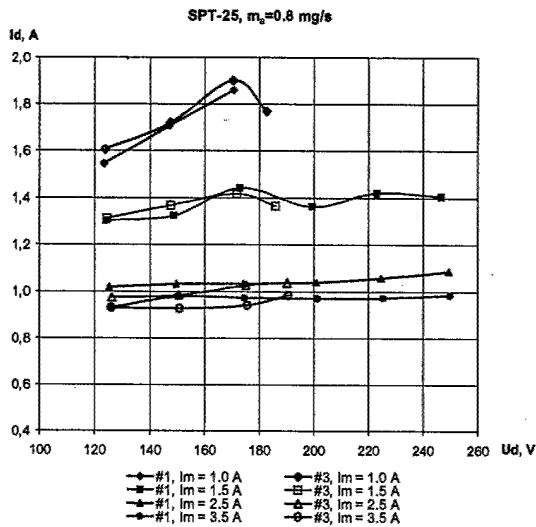American institute of Aeronautics and Astronautics

SPT-25, mₐ=0.6 mg/s

Id, A

Ud, V

—♦—#1, Im = 1.0 A   —♦—#3, Im = 1.0 A
—■—#1, Im = 1.5 A   —☐—#3, Im = 1.5 A
—▲—#1, Im = 2.5 A   —△—#3, Im = 2.5 A
—●—#1, Im = 4.0 A   —○—#3, Im = 4.0 A

Fig. 22. Voltage-current characteristics with discharge chamber exit rings made of BGP (#1) and ABN (#3).

SPT-25, mₐ=0.6 mg/s, Im=2.5 A

T, mN

Ud, V

—▲—#1, Im = 2.5 A   —♦—#3, Im = 2.5 A

Fig. 25. Thrust versus the discharge voltage with discharge chamber exit rings made of BGP (#1) and ABN (#3).

SPT-25, mₐ=0.6 mg/s, Im=1.0 A

T, mN

Ud, V

—▲—#1, Im = 1.0 A   —■—#3, Im = 1.0 A

Fig. 23. Thrust versus the discharge voltage with discharge chamber exit rings made of BGP (#1) and ABN (#3).

SPT-25, mₐ=0.6 mg/s, Im=4.0 A

T, mN

Ud, V

—▲—#1, Im = 4.0 A   —♦—#3, Im = 4.0 A

Fig. 26. Thrust versus the discharge voltage with discharge chamber exit rings made of BGP (#1) and ABN (#3).

SPT-25, mₐ=0.6 mg/s, Im=1.5 A

T, mN

Ud, V

—▲—#1, Im = 1.5 A   —♦—#3, Im = 1.5 A

Fig. 24. Thrust versus the discharge voltage with discharge chamber exit rings made of BGP (#1) and ABN (#3).

SPT-25, mₐ=0.6 mg/s

ηt

Ud, V

—♦—#1, Im = 1.0 A   —♦—#3, Im = 1.0 A
—■—#1, Im = 1.5 A   —☐—#3, Im = 1.5 A
—▲—#1, Im = 2.5 A   —△—#3, Im = 2.5 A
—●—#1, Im = 4.0 A   —○—#3, Im = 4.0 A

Fig. 27. Thrust efficiency versus the discharge voltage with discharge chamber exit rings made of BGP (#1) and ABN (#3).

SPT-25, m_c=0.8 mg/s

Fig. 28. Voltage-current characteristics with discharge chamber exit rings made of BGP (#1) and ABN (#3).

SPT-25, m_c=0.8 mg/s, Im=2.5 A

Fig. 31. Thrust versus the discharge voltage with discharge chamber exit rings made of BGP (#1) and ABN (#3).

SPT-25, m_c=0.8 mg/s, Im=1.0 A
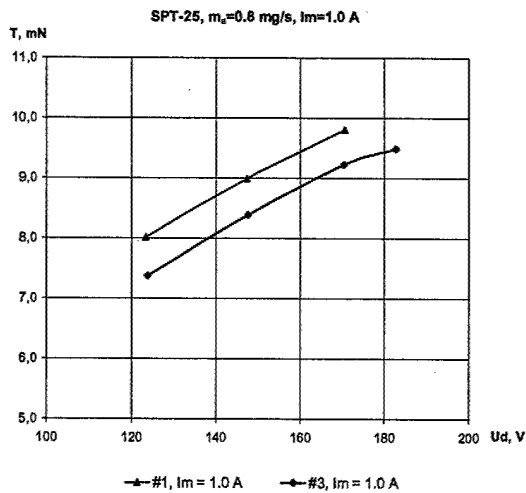

Fig. 29. Thrust versus the discharge voltage with discharge chamber exit rings made of BGP (#1) and ABN (#3).

SPT-25, m_c=0.8 mg/s, Im=3.5 A
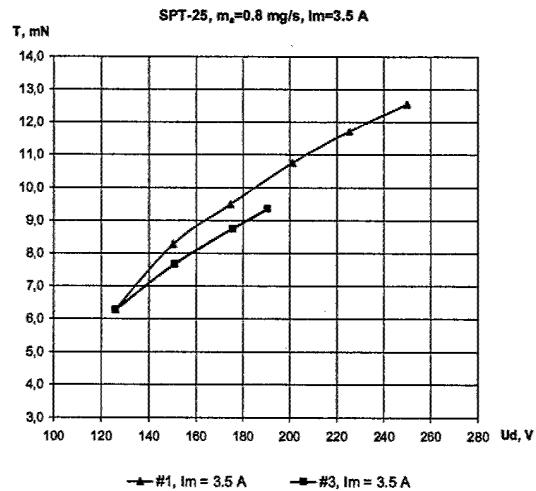

Fig. 32. Thrust versus the discharge voltage with discharge chamber exit rings made of BGP (#1) and ABN (#3).

SPT-25, m_c=0.8 mg/s, Im=1.5 A

Fig. 30. Thrust versus the discharge voltage with discharge chamber exit rings made of BGP (#1) and ABN (#3).

SPT-25, m_c=0.8 mg/s

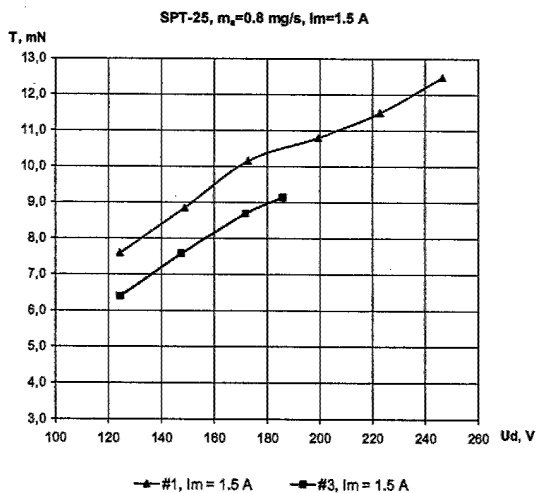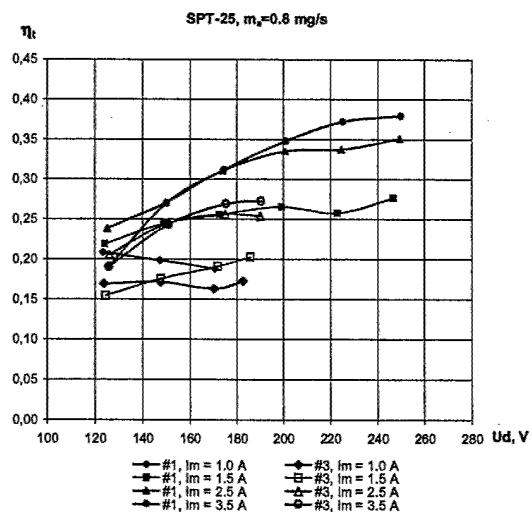Fig. 33. Thrust efficiency versus the discharge voltage with discharge chamber exit rings made of BGP (#1) and ABN (#3).